



April 2011

Compact Power Amplifier for LTE Mobile Terminals Using Coupling Variation Reduction Technique

By Yang Li, Dmitri Prikhodko, Yevgeniy Tkachenko and Rick Zhu, Skyworks Solutions, Inc.

To meet the overwhelming demand for high data rate mobile applications, 3GPP long-term evolution (LTE) is quickly developing around the world as a major step forward in cellular technology. In December 2009, the world's first commercial LTE service opened by TeliaSonera in Stockholm and Oslo. In September 2010, the first US commercial LTE service launched by MetroPCS in Las Vegas and Dallas. On December 5, 2010, Verizon Wireless launched its 4G Band13 LTE network in 38 markets covering 110 million people in the United States and targeting full nationwide coverage in 2013.

Table 1 summarizes world wide LTE frequency bands and the regions in which there is deployment.

Table 1: LTE Frequency Bands and the Corresponding Regions

LTE Bands	Uplink (MHz)	Downlink (MHz)	Duplex Spacing (MHz)	BW (MHz)	Duplex Mode	Deployment in the world
Band 1	1920 -1980	2110 -2170	190	60	FDD	China, Japan, EU, Asia, Australia
Band 2	1850 -1910	1930 -1990	80	60	FDD	North/South America
Band 3	1710 -1785	1805 -1880	95	75	FDD	EU, China, Asia, Australia, Africa
Band 4	1710 -1755	2110 -2155	400	45	FDD	North/South America
Band 5	824 -849	869 -894	45	25	FDD	North/South America, Australia, Asia, Africa
Band 6	830 -840	875 -885	45	10	FDD	Japan
Band 7	2500 -2570	2620 -2690	120	70	FDD	EU, South America, Asia, Africa, Australia
Band 8	880 -915	925 -960	45	35	FDD	EU, South America, Asia, Africa, Australia
Band 9	1749.9 -1784.9	1844.9 -1879.9	95	35	FDD	Japan
Band 10	1710 -1770	2110 -2170	400	60	FDD	North/South America
Band 11	1427.9 -1447.9	1475.9 -1495.9	48	35	FDD	Japan
Band 12	698 -716	728 -746	30	18	FDD	North America
Band 13	777 -787	746 -756	31	10	FDD	North America
Band 14	788 -798	758 -768	30	10	FDD	North America
Band 17	704 -716	734 -746	30	12	FDD	North America
Band 18	815 -830	860 -875	45	15	FDD	North/South America, Australia, Asia, Africa
Band 19	830 -845	875 -890	45	15	FDD	North/South America, Australia, Asia, Africa
Band 20	832 -862	791 -821	41	30	FDD	EU
Band 21	1447.9 -1462.9	1495.9 -1510.9	48	15	FDD	Japan
Band 22	3410 - 3500	3510 - 3600	100	90	FDD	
Band 24	1626.5 -1660.5	1525 -1559	101.5	34	FDD	
Band 33	1900 -1920		N/A	20	TDD	
Band 34	2010 -2025		N/A	15	TDD	China
Band 35	1850 -1910		N/A	60	TDD	
Band 36	1930 -1990		N/A	60	TDD	
Band 37	1910 -1930		N/A	20	TDD	
Band 38	2570 -2620		N/A	50	TDD	EU
Band 39	1880 -1920		N/A	40	TDD	China
Band 40	2300 -2400		N/A	100	TDD	China, Asia
Band 41	2496 -2690		N/A	194	TDD	
Band 42	3400 -3600		N/A	200	TDD	
Band 43	3600 -3800		N/A	200	TDD	

LTE's radio access is called evolved UMTS terrestrial radio access network (E-UTRAN). The air interface of E-UTRAN is based on orthogonal frequency division multiple access (OFDMA) in the downlink (DL), and single carrier frequency division multiple access (SC-FDMA) in the uplink (UL) direction. It supports QPSK and 16QAM. Its bandwidth can be setup as 1.4, 3, 5, 10, 15 and 20MHz. With such complicated radio access and modulation scheme, LTE imposes tough requirements on the PAM designs, especially on its linear power, efficiency and size.

LTE application scenario naturally requires high efficiency to extend battery life in user equipment (UE). However, its SC-FDMA is not really "Single Carrier"; it is essentially a multi-carrier scheme with high peak-to-average power ratio (PAPR). **Table 2** shows the probability based on complementary cumulative distribution function (CCDF) curves for WCDMA, HSDPA, LTE and WiMAX.

Table 2: LTE Frequency Bands and the Corresponding Regions

CCDF	WCDMA Rel99 (dB)	HSDPA (dB)	LTE QPSK 10MHz 12RB (dB)	LTE QPSK 10MHz 50RB (dB)	LTE 16QAM 20MHz 100RB (dB)	WiMAX 16QAM 1024 (dB)
10%	1.7	2.6	2.4	2.3	2.8	3.6
1%	2.4	3.3	4.5	4.4	5.0	6.5
0.1%	2.6	3.5	5.7	5.7	6.4	8.4
0.01%	2.7	3.8	6.5	6.6	7.4	9.5

It can be seen that although PAPR of LTE is lower than OFDM, it is still significantly higher than WCDMA. With a typical test signal 10MHz 12 Resource Blocks QPSK, where maximum power reduction (MPR) is equal to 0dB, its PAPR is approximately 2.8dB higher than the WCDMA signal when CCDF is equal to 0.01%. Higher linearity requirement increases the back off of output power and results in efficiency drop. Reuse of WiMAX PA in LTE can meet linearity requirements, but its PAE is faced with severe challenges from the talk time point of view [3].

LTE UE adopts multi-band and multi-mode solutions. To reduce size and cost, daisy chain architecture is a promising approach for its power control; hence, high directivity coupler is required to maintain small coupling factor variation over output VSWR. Usually, the requirement of the ratio variation should be within $\pm 0.25\text{dB}$, which is very demanding specifications for small form factor PAM.

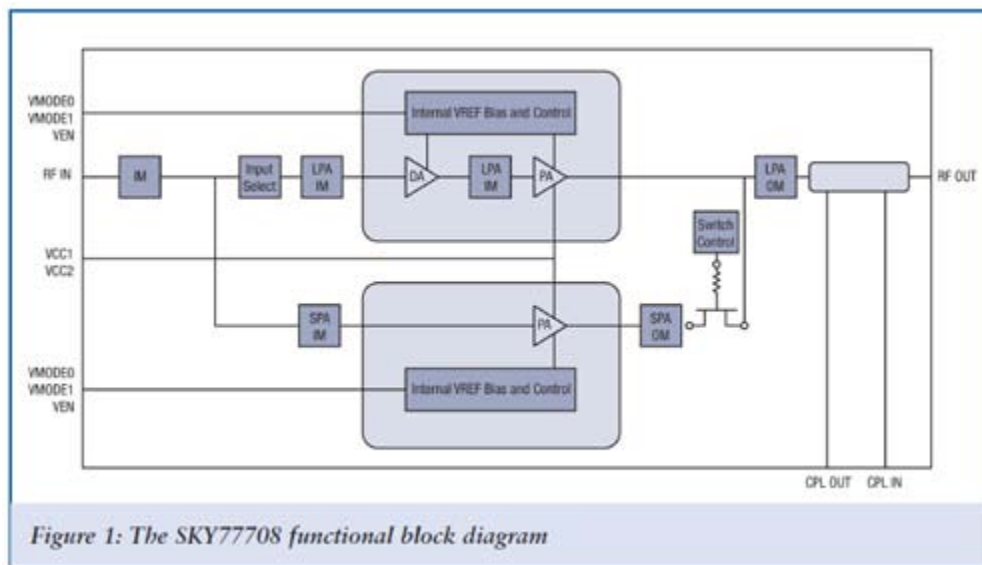


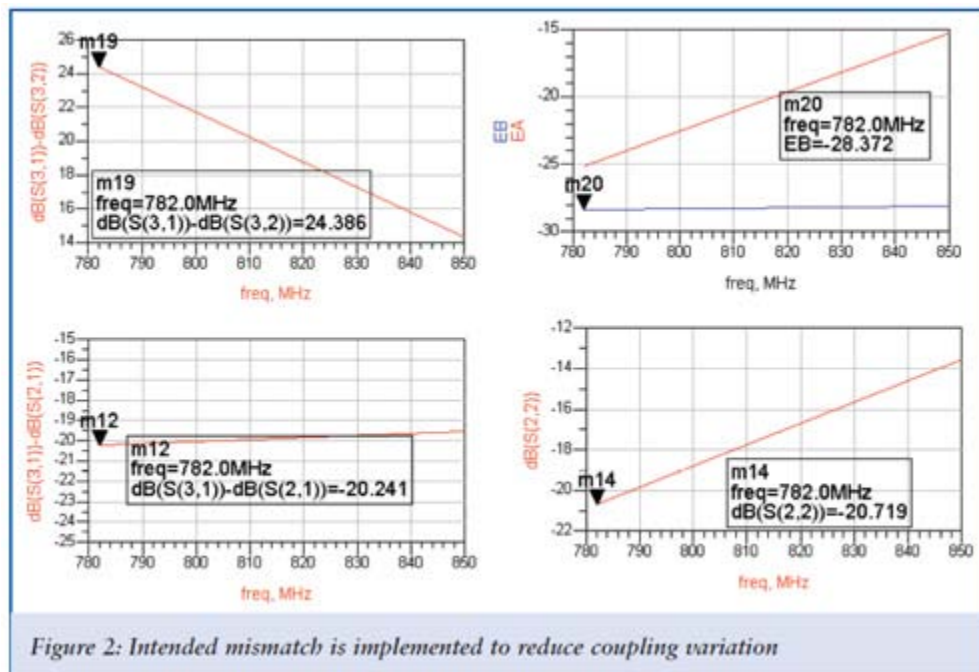
Figure 1: The SKY77708 functional block diagram

A compact Band13 power amplifier module, the SKY77708, is presented, which meets the above stringent requirements. With typical 3.4V supply voltage, it achieves 27.5dBm linear output power in high power mode while keeping UTRAN ACP1 lower than -38dBc and UTRAN ACP2 lower than -50dBc, tested with LTE 10MHz QPSK 12RB signal. Total supply current is typically 470mA at 27.5dBm while gain is about 30dB. Under VSWR 2.5:1, coupling factor variation is only $\pm 0.15\text{dB}$ for both Bands. MMIC PA, matching networks and directional coupler are all integrated into a 3 x 3 mm² package.

Power Amplifier RF Lineup Implementation

To obtain long talk time, high peak PAE is not only desired, but high average PAE is as well which is defined by statistical probability density function (PDF) of output power. Path switching architecture is widely used to realize three power modes PAM and obtain high average PAE. The functional block diagram of the SKY77708 is shown in Figure 1.

There are two parallel paths configuring three power modes: high power mode (HPM), medium power mode (MPM) and low power mode (LPM). In HPM, two stage large PA devices are used to deliver output power up to 27.5dBm while in MPM and LPM, there is smaller size single stage device to cover output power lower than 16dBm. Path switching is implemented by bias and control circuitry as well as switchable matching networks. Two switchable matching networks are at input and output to switch impedances fitting each mode and isolate paths loading effects. In HPM, bias and control circuit turn-on devices in high power path (the top chain) and turn-off devices in medium/low power path (the bottom chain). Meanwhile, it also sets switches in switchable input/output matching networks. Vice versa, in MPM/LPM, devices in medium power/low path are turned on while devices in high power mode are tuned off. MPM and LPM have different bias current, so that lower bias current in LPM can boost PAE at low output power. A high directional coupler is located after the switchable output matching network to sense output power of both modes. It has a coupling factor higher than 20dB and only causes small PAE drop.



Skyworks' BiFET4 InGaP/GaAs HBT technology is adopted to fabricate PAM. The HBT/BiFET process offers single low voltage power supply, FETs, high power density and high efficiency. The developed PAM is optimized for Band 13 which is from 777 MHz to 787 MHz and can also be used in Band 14 covering from 788 MHz to 798 MHz.

The main path of PAM utilizes two gain stages producing 30dB gain across the band. Low pass topology is adopted in both input and output matching networks and high pass topology is used in the inter-stage matching. Two stage output matching networks are used to reduce loss where the first shunt branch tunes harmonics which is essential to optimize efficiency and linearity. RC feedback in drive stage is used to improve stability. Separated bias circuitry to each gain stage is provided and they can be switched ON and OFF by control circuitry.

Intended Mismatched Coupler

Coupler is the critical component in LTE PAM. Its performance is measured by variation range or peak-to-peak error of the coupling factor under VSWR 2.5:1.

Traditionally, high directivity is required to obtain small peak-to-peak error. To obtain peak-to-peak error smaller than 0,5dB, directivity should exceed 23dB [9].

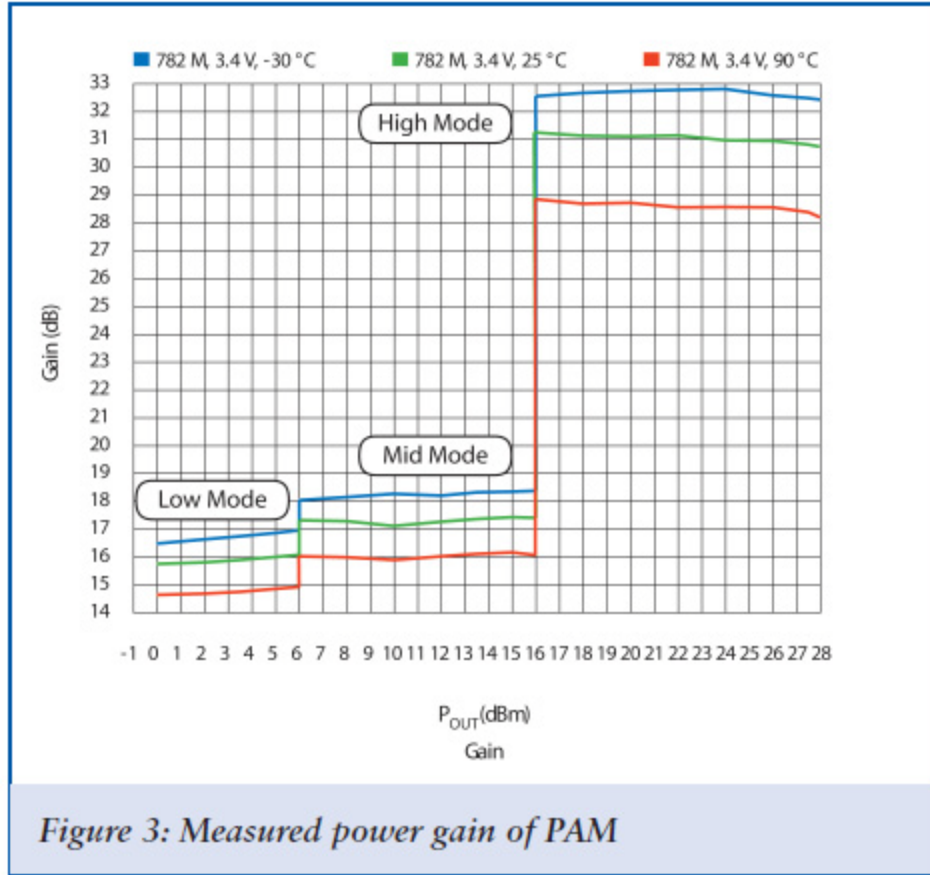


Figure 3: Measured power gain of PAM

Theoretical analysis shows that a coupled strips coupler can be ideally matched and perfectly isolated, if its inductive coupling coefficient equals to the capacitive one. However, meeting this condition requires layout symmetry along coupler arm direction and proper permittivity of substrate material. In current PAM designs, dielectric constant is mostly determined by laminate technology and symmetry requirements of coupler arms cannot be met when clearance is insufficient in compact packaging design. This coupler's specification is becoming more demanding while PAM size is reduced to 3 x 3 mm.

To reduce coupling variation in such small module, intended mismatch at output port of main arm is realized. The principle can be explained mathematically. In PAM design, coupler performance requirements are specified by coupling factor C_{pout} , and coupling factor variation or peak-to-peak error P_k .

$$C_{pout} = \frac{P_{out}}{P_c}$$

Equation 1

$$P_k = \max(\Delta C_{pout})|_{VSWR}$$

Equation 2

We define Γ_L as the load impedance normalized to 50Ohm, S_{ij} as the coupler's S parameter under matched condition and assume $S_{33}=S_{44}=0$. The following equation can be derived,

$$C_{port} = \frac{|S_{21}| \sqrt{(1-|\Gamma_L|^2)}}{|S_{31}| \left| 1 + \left(\frac{S_{21}S_{32}}{S_{31}} - S_{22} \right) \Gamma_L \right|}$$

Equation 3

$$Pk_{dB} = 20 \log_{10} \frac{\left| 1 + \left(\frac{S_{21}S_{32}}{S_{31}} - S_{22} \right) \Gamma_L \right|}{\left| 1 - \left(\frac{S_{21}S_{32}}{S_{31}} - S_{22} \right) \Gamma_L \right|}$$

Equation 4

When output port is not perfectly matched, let's define equivalent directivity,

$$D = \left| \frac{1}{\frac{S_{32}}{S_{31}} - \frac{S_{22}}{S_{21}}} \right|$$

Equation 5

When output port is perfectly matched, the directivity becomes,

$$D = \left| \frac{S_{31}}{S_{32}} \right|$$

Equation 6

This is the same as traditional coupler directivity definition. Then, Equation 4 becomes:

$$Pk_dB = 20 \log_{10} \left| \frac{1 + \frac{S_{21}}{D} \Gamma_L}{1 - \frac{S_{21}}{D} \Gamma_L} \right|$$

Equation 7

It is clear that the higher D, the better Pk.

When a coupler's directivity is limited by coupler size or cross-coupling between coupler and other traces, Equation 5 shows that adjusting amplitude and phase of Sij to cancel part of S32 / S31 will improve equivalent directivity.

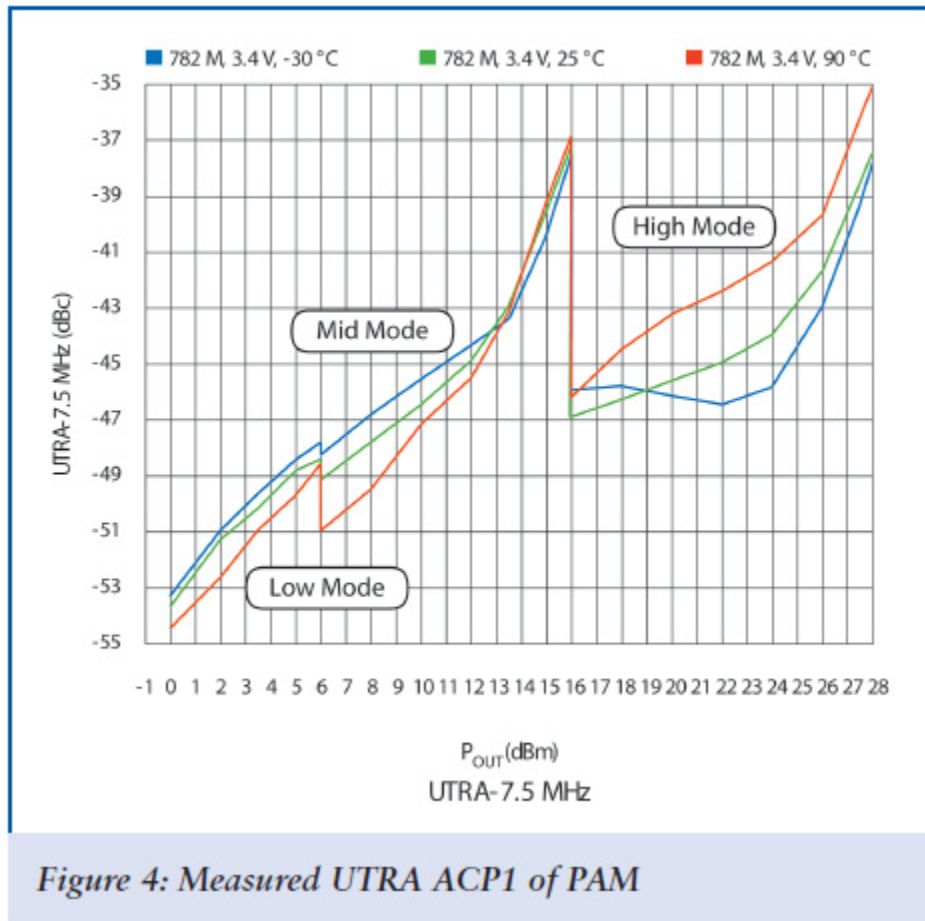


Figure 4: Measured UTRA ACP1 of PAM

In the SKY77708, a discontinuity is created to obtain -20.7dB output return loss and improves coupler directivity from 24.4dB to 28.4dB, as shown in **Figure 3**.

Peak-to-peak error measurement of the PAM with VSWR 2.5:1 shows 0.3dB variation at Band 13 is achieved, which is the variation expected by a well matched 28dB coupler.

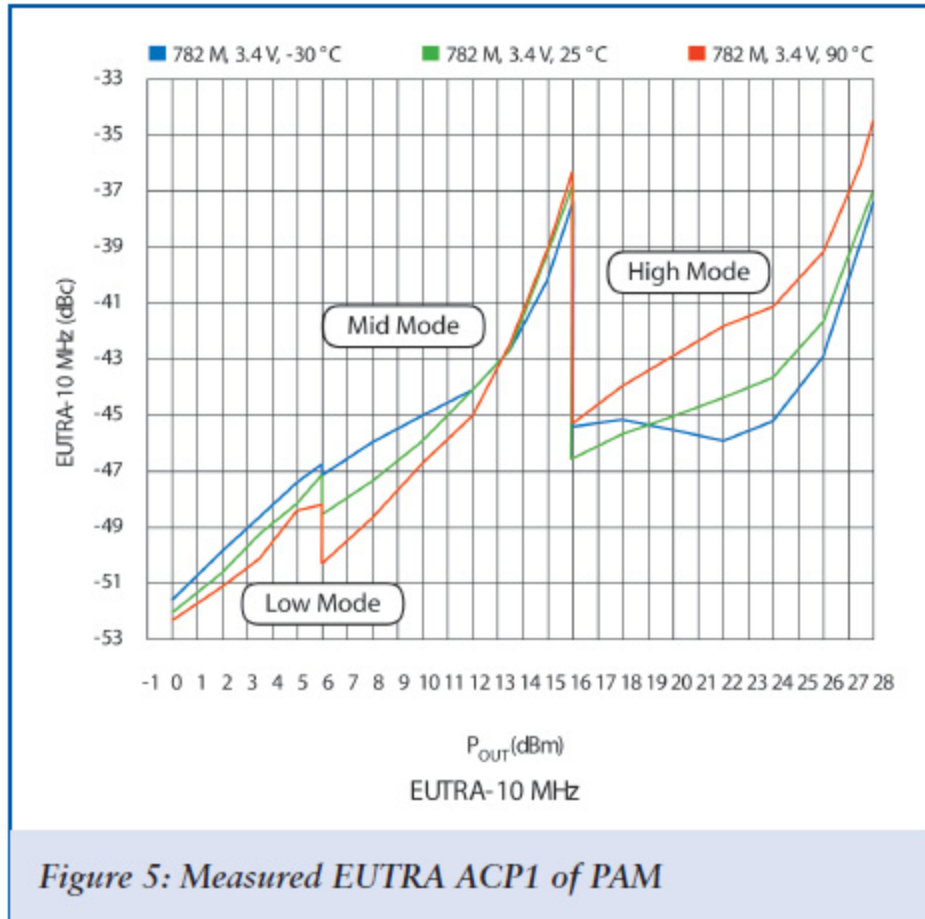


Figure 5: Measured EUTRA ACP1 of PAM

In practical design, the output matching networks is close to the coupler and coupling between them causes dependency of S parameter of the coupler on matching components. In order to both minimize this coupling and optimize the output matching network, we have carried out 3D EM simulations.

Measurements Results

We now present measurement results of the FR4 test board with LTE 10MHz 12RB QPSK signal and 3.4V power supply.

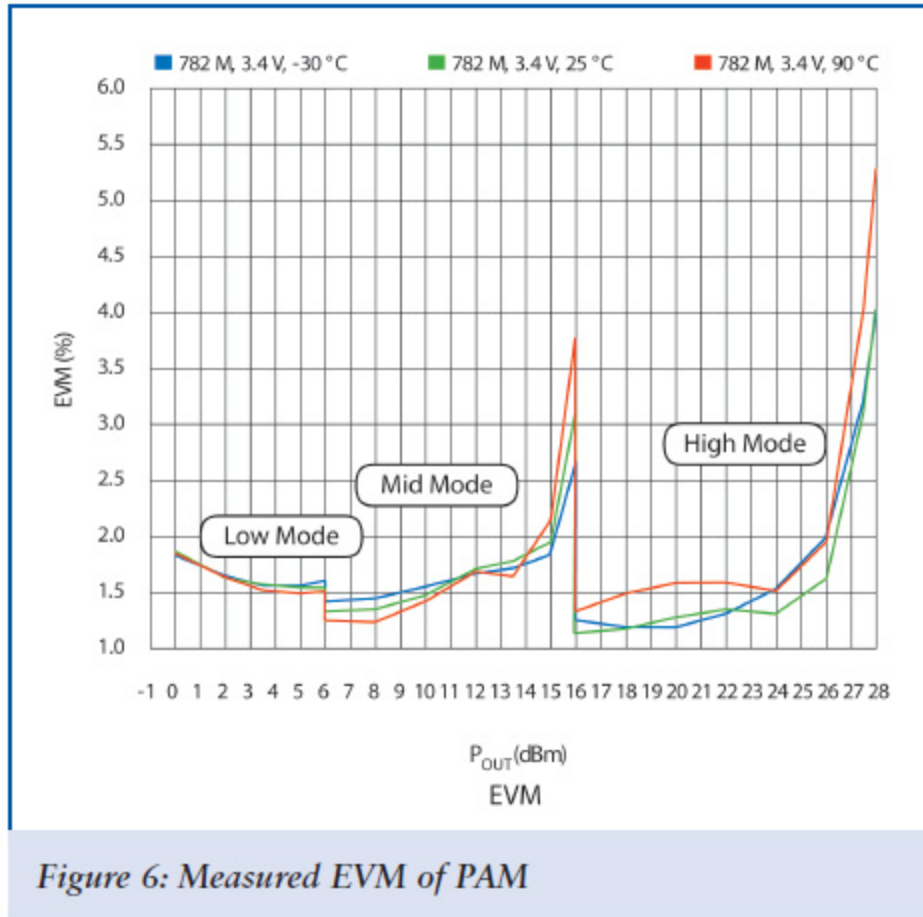


Figure 6: Measured EVM of PAM

Figure 3 is measured gain of the PAM for three power modes and at -30°C, 25°C and 90°C. The typical gain is higher than 30dB in HPM, and 17dB in MPM at room temperature.

ACP and EVM characteristics are illustrated in **Figure 4**, **Figure 5** and **Figure 6**. At the room temperature, ACP1 in UTRA is expected lower than -38dBc, ACP1 in EUTRA is lower than -36dBc and EVM is lower than 3.5 percent until 27.5dBm.

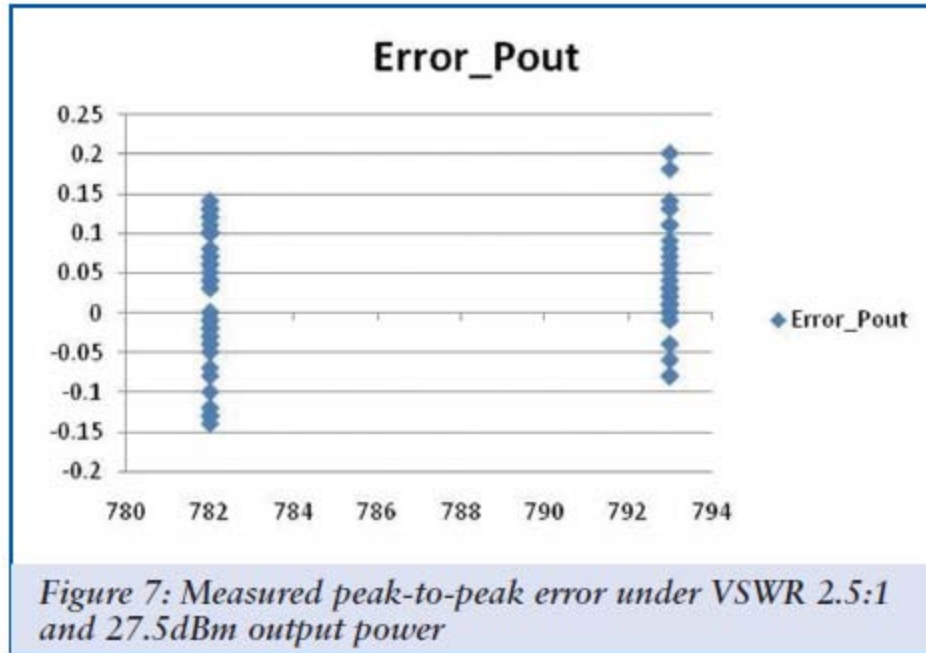


Figure 7 shows Peak-to-Peak Error of coupling factor under VSWR 2.5:1 vs. phase. ± 0.15 dB is achieved at Band 13. At Band 14, the coupling variation is $+0.22$ dB/ -0.1 dB.

Conclusion

We have developed a compact high efficiency dual power modes PAM for Band13 LTE applications. With 3.4V power supply, it achieves 27.5dBm output power while meeting -39dBc Ultra ACP1. High directive coupler is integrated to realize 0.3dB peak-to-peak error under VSWR 2.5:1. A complete PA module is packaged on an area of 3 x3 mm.

References

- [1] 3GPP TS 36.101-v8.5.1, E-UTRA user equipment radio transmission and reception.
- [2] H.G. Myung, Junsung Lim, D.J. Goodman, "Single carrier FDMA for uplink wireless transmission." *Vehicular Technology Magazine, IEEE.*, vol. 1, issue 3, pp. 30-38, Sep 2006.
- [3] Y.H. Chow, C.K. Yong, J. Lee, H.K. Lee, J. Rajendran, S.H. Khoo, M.L. Soo, C.F. Chan, "A variable supply, (2.3;2.7) GHz linear power amplifier module for IEEE 802.16e and LTE applications using E-mode pHEMT technology." *2008 IEEE MTT-S Int. Microwave Symp. Dig.*, pp. 871-874, June 2008.
- [4] G. Hau, J. Turpel1, J. Garrett, H. Golladay, "A WCDMA HBT Power Amplifier Module with Integrated Si DC Power Management IC for Current Reduction under Backoff Operation." *2007 RFIC Symposium*, pp. 75-78, June 2007.
- [5] Joon Hyung Kim, Ji Hoon Kim, Noh, Y.S. Chul Soon Park, "An InGaP-GaAs HBT MMIC smart power amplifier for WCDMA mobile handsets." *IEEE Journal of Solid-state Circuits.*, vol. 38, no. 6, pp. 905-910, June 2003.
- [6] T.Y. Yum, Chiu Leung, Hou Chan Chi, Quan Xue, "High-efficiency linear RF Amplifier - a unified circuit approach to achieving compactness and low distortion." *IEEE Trans. Microwave Theory & Tech.*, vol. 54, no. 8, pp. 3255-3266, August 2006.
- [7] G. Zhang, S. Chang, A. Wang, "WCDMA PCS Handset Front End Module." *2006 IEEE MTT-S Int. Microwave Symp. Dig.*, pp. 304-307, June 2006.
- [8] C. J. Wei, A. Metzger, Y. Zhu, C. Cismaru, A. klimashov, Y. A. Tkachenko, "Four Terminal GaAs-InGaP BiFET DC model for wireless application." *2005 APMC Microwave Conference Proceedings*, Dec 2005.
- [9] Y. Li, R. Zhu, D. Prikhodko, Y. Tkachenko, "LTE power amplifier module design: Challenges and trends" *IEEE International Conference on Solid-State and Integrated Circuit Technology (ICSICT)*, Nov 2010.